Lukáš KOUDELA, Václav KOTLAN, Ivo DOLEŽEL

University of West Bohemia, Pilsen, Czech Republic

Monolithic model of induction shrink fit for high-speed tools

Abstract. *Axisymmetric induction clamping of high-speed machine tools is proposed and modeled. The model consists of three nonlinear partial differential equations (PDEs) describing the distribution of magnetic field, temperature field and field of thermoelastic displacements in the domain. The system is solved numerically in the monolithic formulation using own code Agros2D based on a fully adaptive higher-order finite element method. The methodology is illustrated with an example of fixing the shank of a high-revolution drilling tool in the clamping head.*

Streszczenie. *W artykule zaproponowano I zamodelowano osiowo-symetryczne zaciskanie w wysokoobrotowych maszynach. Model składa się z trzech nieliniowych cząstkowych równań różniczkowych, opisujących rozkład pola magnetycznego, pola temperatury i pola odkształceń termoplastycznych. Układ równań rozwiązywany jest numerycznie w sformułowaniu monolitycznym z wykorzystanie własnego oprogramowania Agross2D opartego na adaptacyjnej wyższego rzędu metodzie elementów skończonych. Przedstawiona metodologia została zilustrowana przykładem dopasowania trzonu wysokoobrotowej wiertnicy w głowicy zaciskowej. (**Monolityczny model ściskania indukcyjnego w maszynach z dużą prędkością**)*

Keywords: induction shrink fit, magnetic field, temperature field, field of thermoelastic displacements, monolithic formulation.
Słowa kluczowe: ściskanie indukcyjne, pole magnetyczne, pole odkształceń termoplastycznych, sformułowanie monolityczne

doi:10.12915/pe.2014.12.31

Introduction

Induction clamping is a hot-pressing technology, where heat is produced by induction heating [1]. Its typical representatives are induction shrink fits used for clamping high-revolution tools, for example, in the automotive and aerospace industries [2–3].

The process of assembly of a shrink fit is depicted in Fig. 1. At cold, the diameter of the bore of the clamping head is d_1 and diameter of the tool shank is $d_2 > d_1$ (Fig. 1, upper part). First, the clamping head must be heated (by induction) as long as the dilatation of its bore δ allows inserting the shank of a prescribed length into the bore (which means, that along the length of the bore $d_3 > d_2$, Fig. 1, bottom part). The system is then intensively cooled, which produces the shrink fit. At the end of the process, both the hole and shank have the same diameter d_4, for which $d_1 < d_4 < d_2$. When the shank is not considered elastic (after the pressure its diameter remains the same), then $d_4 = d_2$.

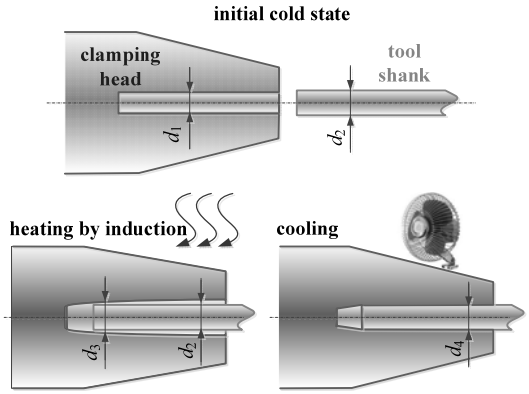

Fig. 1. Induction clamping - shank tool is inserted into heated clamping head and system is cooled

The parameters of the shrink fit must be derived from the mechanical torque to be transferred. Its disassembly is realized in a similar manner. The important condition is that the material of the clamping head is made of material with a substantially higher thermal dilatability than the material of the tool shank.

The induction clamping technology exhibits, with respect to other existing clamping technologies, numerous advantages. We can mention, for example:

- quality of balance of the shank,
- minimum eccentricity due to the rotating runout,
- high clamping force and dynamic stiffness at high torques,
- simplicity of the whole system,
- and a long life expectancy (obvious from Fig. 2).

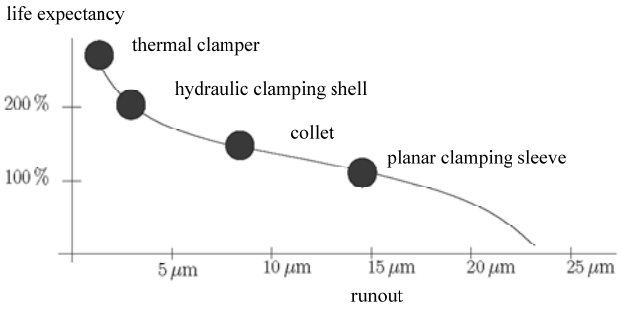

Fig. 2. Runout and life expectancy of particular ways of clamping

Formulation of the technical problem

The task is to propose the induction shrink fit for clamping a high-revolution drilling tool in the head. The materials of both the tool shank and clamping head are known. The clamping head was purchased from the company Gühring [4] that belongs to one of the leading European manufacturers of this technology. It is depicted in Fig. 3 and its principal dimensions follow from Fig. 4. The material parameters are known, together with their temperature dependences.

Fig. 3. View of investigated clamping head

The first task is to propose the minimum diameter d_2 of the tool shank so that the system clamping head-drilling tool is able to transfer the prescribed mechanical torque M_{start}. The next step is to propose the inductor and parameters of the field current such that they allow heating of the clamping head in an acceptable time (5–15 s) to increase the bore

diameter to $d_3 > d_2$ along the whole length l of its left part (see Fig. 4). The third task is to map the process of induction heating.

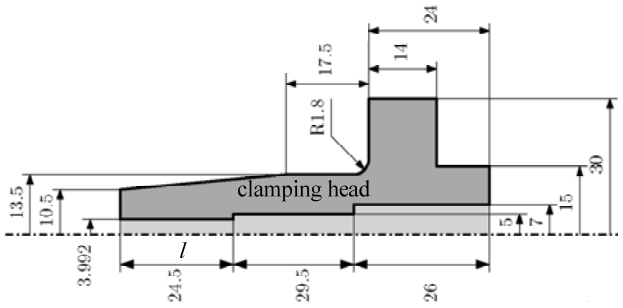

Fig. 4. Principal geometrical dimensions of head (in mm)

Mathematical model

The system may be (with a small inaccuracy) considered axi-symmetric, which strongly simplifies the situation. First, we have to determine the interference δ between the radius $d_1/2$ of the bore and radius $d_2/2$ of the tool shank, see Fig. 5.

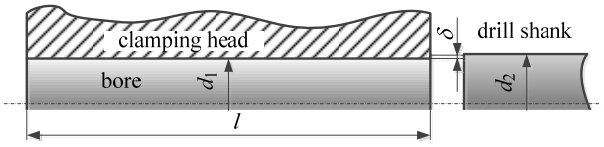

Fig. 5. Relation between interference δ and starting mechanical torque M_{start}

After heating the clamping head and inserting there the drill shank of length l the pressure between both parts is given by the formula

$$p = \frac{\delta E}{d_1} \cdot \frac{d_2^2 - d_1^2}{d_2^2} \tag{1}$$

and this pressure must satisfy the condition

$$p \cdot \frac{d_2^2}{d_2^2 - d_1^2} = \frac{\delta E}{d_1} \le \frac{\sigma_a}{4}, \tag{2}$$

where E denotes the Young modulus of the corresponding material and σ_a is its allowable mechanical stress. The starting mechanical torque M_{start} then follows from the expression

$$M_{\text{start}} = \pi \frac{d_1^2}{2} p l f_f = \pi \frac{d_1^2}{2} \frac{\delta E}{d_1} \cdot \frac{d_2^2 - d_1^2}{d_2^2} l f_f \approx 2\pi \delta^2 E l f_f, \tag{3}$$

where f_f is the coefficient of dry friction between the materials of the clamping head and tool shank.

The process of induction heating will be first described by its continuous mathematical model. This model consists of three partial differential equations (PDEs) providing the distribution of the magnetic field, temperature field, and field of thermoelastic displacements in the system.

The magnetic field can (in the axisymmetric 2D arrangement), see Fig. 6, be advantageously described by the parabolic PDE for the magnetic vector potential $\boldsymbol{A}$ in the form [5]

$$\operatorname{curl}\left(\frac{1}{\mu}\operatorname{curl}\boldsymbol{A}\right) + \gamma\frac{\partial \boldsymbol{A}}{\partial t} = \boldsymbol{J}_{\text{ext}}, \tag{4}$$

where μ denotes the magnetic permeability, γ stands for the electric conductivity and $\boldsymbol{J}_{\text{ext}}$ is the vector of the external harmonic current density in the field coil. But solution to (4) is, in this particular case, practically unfeasible. The reason consists in the deep disproportion between the frequency f (usually thousands Hz) of the field current I_{ext} and time of heating t_H (more seconds). That is why the model was somewhat simplified using the assumption that the magnetic field is harmonic. In such a case it can be described by the Helmholtz equation for the phasor $\underline{\boldsymbol{A}}$ of the magnetic vector potential $\boldsymbol{A}$ [6]

$$\operatorname{curlcurl}\underline{\boldsymbol{A}} + \mathrm{j}\cdot\omega\gamma\mu\underline{\boldsymbol{A}} = \mu\underline{\boldsymbol{J}}_{\text{ext}}. \tag{5}$$

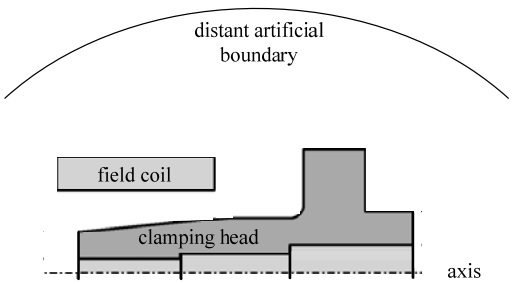

Fig. 6. Definition area of magnetic field

Here, ω denotes the angular frequency ($\omega = 2\pi f$). But the magnetic permeability μ of ferromagnetic parts is supposed not to be a constant; it is always assigned to the local value of magnetic flux density. Its computation is, in such a case, based on an appropriate iterative procedure.

The conditions along the axis of the system and artificial boundary placed at a sufficient distance from it are of the Dirichlet type ($\underline{\boldsymbol{A}} = \underline{\boldsymbol{0}}$).

The temperature field T in the clamping head is described by the heat transfer equation [7]

$$\operatorname{div}(\lambda \cdot \operatorname{grad} T) = \rho c_p \cdot \frac{\partial T}{\partial t} - w, \tag{6}$$

where λ is the thermal conductivity, ρ denotes the mass density and c_p stands for the specific heat (all of these parameters are generally temperature-dependent functions). Finally, symbol w denotes the time average internal volumetric sources of heat that generally consist of the volumetric Joule losses w_J (due to eddy currents) and magnetization losses w_m. Thus, we can write

$$w = w_J + w_m, \tag{7}$$

where

$$w_J = \frac{\left|\underline{\boldsymbol{J}}_{\text{eddy}}\right|^2}{\gamma}, \quad \underline{\boldsymbol{J}}_{\text{eddy}} = -\mathrm{j}\cdot\omega\gamma\underline{\boldsymbol{A}}, \tag{8}$$

while w_m are determined from the known measured loss dependence $w_m = w_m(|\underline{\boldsymbol{B}}|)$ for the material used (magnetic flux density $\boldsymbol{B}$ in every element is in this model also harmonic), or from the Steinmetz formula In many cases, however, the magnetization losses are neglected as their value is very small with respect to the Joule losses. The boundary conditions take into account convection and radiation.

Finally, the solution of the thermoelastic problem is solved by means of the Lamé non-isothermic equation in the form [8]

$$(\varphi + \psi)\cdot\operatorname{grad}(\operatorname{div}\boldsymbol{u}) + \psi\cdot\Delta\boldsymbol{u} - (3\varphi + 2\psi)\cdot\alpha_T\cdot\operatorname{grad}T = \boldsymbol{0}, \tag{9}$$

$$\varphi = \frac{\nu\cdot E}{(1+\nu)(1-2\nu)}, \quad \psi = \frac{E}{2\cdot(1+\nu)}.$$

Here, E denotes the Young modulus of elasticity of the material, ν is the Poisson coefficient of the contraction,

symbol $\boldsymbol{u}$ represents the vector of the displacements, and $\boldsymbol{f}_{\mathrm{L}}$ stands for the vector of the volumetric forces (it includes the Lorentz forces and gravitational forces, but with respect to the forces of the thermoelastic origin they are usually low and often can be neglected). Finally, α_{T} is the coefficient of the linear thermal dilatability of the material. The boundary conditions correspond to the free clamping head, whose axis is fixed.

It is important to notice that all physical parameters of material of the clamping head ($\mu, \gamma, \lambda, \rho c_{\mathrm{p}}, \alpha_{\mathrm{T}}$) are generally temperature-dependent non-linear functions. That is why the problem of induction heating of the clamping head characterised by the interaction of the the above three fields should be solved in the hard-coupled formulation.

Numerical solution

The numerical solution is carried out in the monolithic formulation, with respect to all mentioned nonlinearities (saturation curve and temperature dependences of material properties). The computations are performed by own code Agros2D [9], [10] based on a fully adaptive higher-order finite element method and tightly cooperating with the library Hermes [11] containing the most advanced procedures for numerical processing. Both codes written in C++ are freely distributable under the GNU General Public License. The most important and in some cases quite unique features of the codes follow:

- Solution of the system of PDEs is carried out monolithically, the resultant numerical scheme is characterized by just one stiffness matrix.
- Fully automatic *hp*-adaptivity. When adaptivity is required, in every iteration step the solution is compared with the reference solution (realized on an approximately twice finer mesh), and the distribution of error is then used for selection of candidates for adaptivity.
- Each physical field can be solved on quite a different mesh that best corresponds to its typical features. In non-stationary processes every mesh can change in time, in accordance with the real evolution of the corresponding physical quantities.
- Easy treatment of the hanging nodes appearing on the boundaries of subdomains whose elements have to be refined. These nodes bring about a considerable increase of the number of the degrees of freedom (DOFs).
- Curved elements able to replace curvilinear parts of any boundary by a system of circular or elliptic arcs. These elements mostly allow reaching highly accurate results near the curvilinear boundaries with very low numbers of the DOFs.

In the course of solution, attention is paid to all important numerical aspects (mainly the convergence and accuracy of the results). The computation of one example takes about 30 minutes on a top-quality PC.

Illustrative example

The solved arrangement is depicted in Fig. 7. The clamping head is made of special tool steel. The position of the inductor with respect to the clamping head is characterized by the shift Δz that can vary.

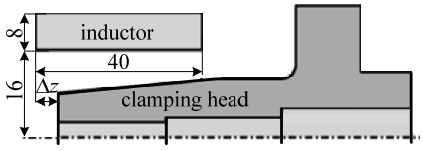

Fig. 7. Position of inductor (other dimensions of system in mm are shown in Fig. 4)

The Young modulus of the material $E = 2.1 \times 10^{11}$ Pa, the Poisson coefficient $\nu = 0.3$, the length of mutual contact between the shank and clamping head $l = 24.5 \times 10^{-3}$ mm, and the coefficient of dry friction $f_{\mathrm{f}} = 0.55$. The value of the interference δ was considered 0.05 mm. The acceptable time of heating $t_{\mathrm{h}} = 5$ s and prescribed $M_{\mathrm{start}} = 12$ Nm.

Important are also the saturation curve and temperature dependences of the material parameters of the considered tool steel. Some are depicted in Figs. 8–9. Figure 8 (left part) shows the saturation curve at the room temperature, while its right part depicts its temperature correction and Fig. 9 depicts the temperature dependencies of electric conductivity γ (left) and thermal conductivity λ (right).

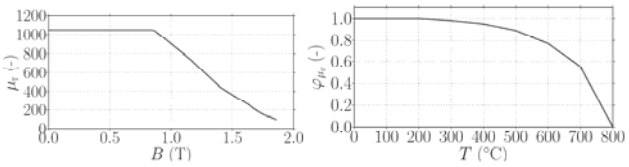

Fig. 8. Saturation curve of tool steel at room temperature (left) and its temperature correction (right)

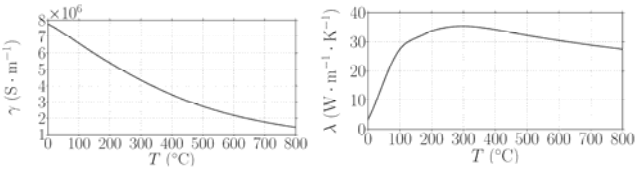

Fig. 9. Temperature dependence of electric conductivity (left) and thermal conductivity (right)

For these material parameters we tested the solution of the problem for varying values Δz, effective value I of the field current and its frequency f. The number of results abound. That is why only selected results for current density $J_{\mathrm{ext}} = 7 \times 10^6$ Am^{-2} will be discussed. All computations were carried out in the monolithic formulation (which means that we respected all the above non-linearities and all three fields were calculated simultaneously).

First, we tested the convergence of the distribution of magnetic field on the density of the discretization mesh and position of the distant artificial boundary (see Fig. 6). It was found the minimum number of non-uniformly distributed elements must be about 33 000, and the radius of the artificial boundary 0.15 m.

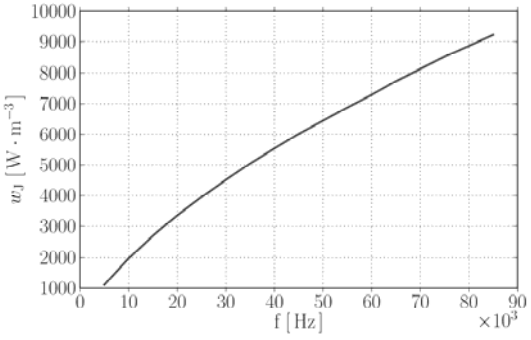

Fig. 10. Average volumetric Joule losses w_{J} in the clamping head versus frequency f ($J_{\mathrm{ext}} = 7 \times 10^6$ Am^{-2})

Figure 10 shows the average value of the Joule losses w_{J} in the clamping head as a function of frequency. Even when for higher frequencies the surface layer where these losses are produced becomes thinner and thinner, the

volumetric losses increase substantially faster and the function grows. With respect to practical possibilities (availability of the field current sources), we decided for the frequency $f = 50$ kHz that is often used in similar heat-treatment technologies.

The distribution of the temperature field (that was only evaluated in the clamping head) converged for about 14 000 second-order elements. Approximately the same holds for the field of thermoelastic displacements. Figure 11 shows the time evolution of the temperature along the internal bore of the clamping head for $\Delta z = 0$, $f = 50$ kHz, and $J_{\text{ext}} = 7 \times 10^6$ Am^{-2}. Finally, Fig. 12 depicts the corresponding time evolution of the radial displacement of the internal bore. For $t_{\text{h}} = 5$ s of heating, however, the minimum displacement reaches the value (light blue line) $\delta = 0.0139$ mm and, hence (see (3)), $M_{\text{start}} = 3.43$ Nm, which is insufficient.

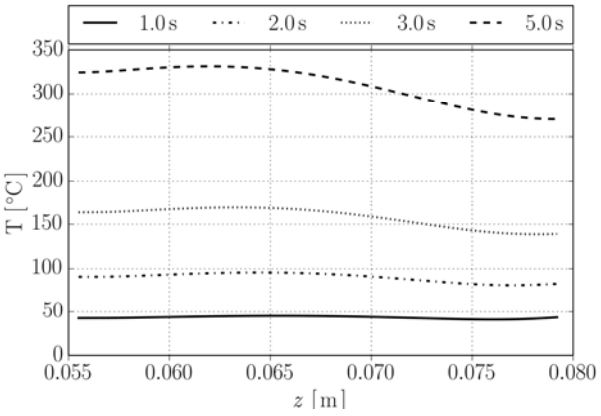

Fig. 11. Evolution of temperature T along internal bore of clamping head ($\Delta z = 0$, $f = 50$ kHz, and $J_{\text{ext}} = 7 \times 10^6$ Am^{-2})

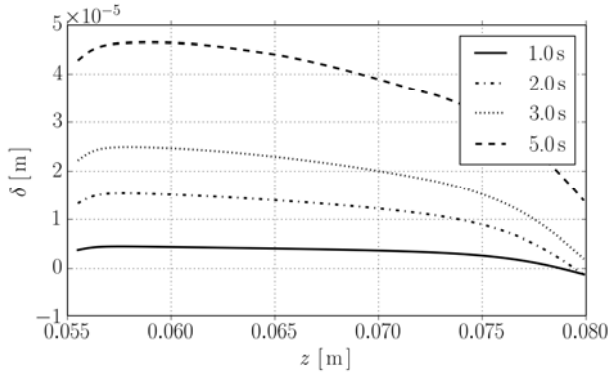

Fig. 12. Evolution of displacements δ along internal bore of clamping head ($\Delta z = 0$, $f = 50$ kHz, and $J_{\text{ext}} = 7 \times 10^6$ Am^{-2})

The first attempt how to increase the interference δ and starting mechanical torque M_{start} was to change the value of Δz (giving the position of the inductor with respect to the clamping head, see Fig. 7). Figure 13 depicts the distribution of displacements after $t_{\text{h}} = 5$ s of heating on this value.

Now it can be seen that for $\Delta z = 0.01$ m the displacements along the whole bore exceed the value $\delta = 0.0282$ mm. The corresponding value of the starting mechanical torque is now $M_{\text{start}} = 14.14$ Nm, which is greater than the required value 12 Nm.

Conclusion

The paper presents a complete mathematical model of an induction shrink fit and method of its numerical solution in the monolithic formulation. The results are promising and correspond to the industrial practice. Next work in the domain must be aimed at the shape optimization of the inductor and its equipment with a suitable focusator of magnetic flux in order to increase the efficiency of the process. The acceleration of computations is crucial as well, particular variants take tens of seconds of the computing time. Planned are also some appropriate experiments. Very important is the question of materials (using materials with a higher dilatability allows transferring higher mechanical torques, on the other hand this property must also be attuned with other material parameters, mostly with its Young modulus and allowable mechanical stress).

Another innovative process is also considered, consisting in induction heating of rotating clamping head in stationary magnetic field produced by suitably distributed high-parameter permanent magnets. The first results are very promising.

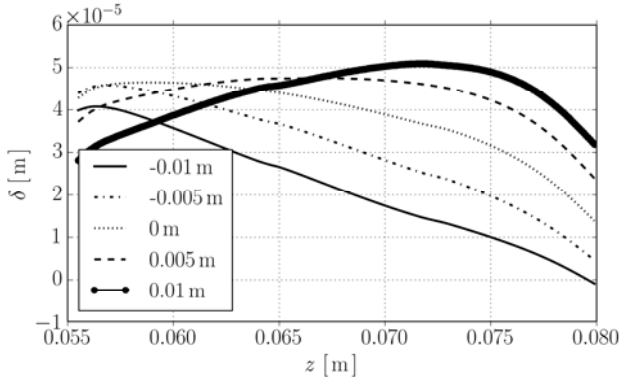

Fig. 13. Distribution of displacements δ along the internal bore of the clamping head after 5 s of heating for varying value of Δz (f = 50 kHz, and $J_{\text{ext}} = 7 \times 10^6$ Am^{-2})

Acknowledgements

The financial support from the project SGS-2012-039 (University of West Bohemia in Pilsen) and project P102/11/0498 (The Grant Agency of the Czech Republic) is highly acknowledged.

REFERENCES

[1] V. I. Rudnev, D. Loveless, R. Cook, M. Black, Handbook of induction heating, CRC Press, Boca Raton, (2002).
[2] Haimer GmbH, URL: http://www.haimer.biz/fileadmin/assets/downloads/kataloge/2014-03_Power_Clamp_Sys-tem_DE-EN_screen.pdf.
[3] Komet Group, URL: http://www.kometgroup.com/pdf/kompass/KomPass_GB.pdf#page=394.
[4] Gühring Ltd., URL: http://www.guehring.cz/data/produkty/GM300_cs.pdf.
[5] M. Kuczmann and A. Iványi The finite element method in magnetics, Akadémiai Kiadó, Budapest, 2008.
[6] J. A. Stratton, Electromagnetic theory, Wiley-IEEE Press, New York, 2007.
[7] J. P. Holman, Heat transfer, McGraw-Hill, New York, 2002.
[8] B. Boley, J. Weiner, Theory of thermal stresses, NY, 1960.
[9] P. Karban, F. Mach, P. Kůs, D. Pánek, I. Doležel (2013) "Numerical solution of coupled problems using code Agros2D", *Computing*, Vol. 95, No. 1, Supplement, pp. 381–408.
[10] P. Karban and others Agros2D - C++ application for the solution of PDEs. URL: http://agros2d.org.
[11] P. Solin and others, Hermes - Higher-order modular finite element system (User's guide). URL: http://hpfem.org.

***Authors**: Ing. Lukáš Koudela, Ing. Václav Kotlan, Ph.D., Prof. Ing. Ivo Doležel, CSc., University of West Bohemia, Univerzitní 26, 306 14 Plzeň, Czech Republic, {koudela, vkotlan, idolezel}@kte.zcu.cz.*